Available at www.sciencedirect.com

ScienceDirect

journal homepage: www.elsevier.com/locate/he

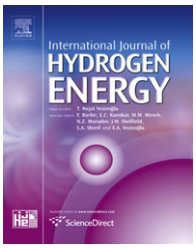

# A combined system of dimethyl ether (DME) steam reforming and lean NOx trap catalysts to improve NOx reduction in DME engines

*Syungyong Park* [a], *Byungchul Choi* [b,*], *Byeong-Soo Oh* [b]

[a] *Graduate School of Mechanical Engineering, Chonnam National University, 300 Yongbong-dong, Gwangju 500-757, Republic of Korea*
[b] *School of Mechanical Systems Engineering, Chonnam National University, 300 Yongbong-dong, Gwangju 500-757, Republic of Korea*

ARTICLE INFO

*Article history:*
Received 7 January 2011
Received in revised form
18 February 2011
Accepted 24 February 2011
Available online 29 March 2011

*Keywords:*
DME steam reforming
Hydrogen
Nitrogen oxide
Lean NOx trap
Exhaust gas
Catalyst

ABSTRACT

This paper performs a study on a combined system of DME steam reforming (SR) and lean NOx trap (LNT) in order to improve the performance of the de-NOx catalyst in DME engines. A new concept, a combined system of SR and LNT catalysts, utilizes $H_2$ and CO generated from the DME SR catalyst as a reductant for the LNT catalyst. The Cu-based SR catalyst was prepared by the sol-gel method; further, the LNT catalyst was used a commercial catalyst. The parameters considered in this experiment included the particle size, dispersion, and amount of Cu loaded on the SR catalyst, the cell density of the substrate of the SR catalyst, and the amount of Zn as a promoter. The experiments revealed that the highest NOx conversion was obtained in the LNT catalyst when the concentration of DME was 1% and the lean/rich time was 55/8 s; however, we decided to supply 0.7% of DME and use 55/5 s of lean/rich time in the combined system of SR and LNT to overcome the problems of DME slip and fuel penalties. The system showed the best performance regarding NOx conversion in the combined system of SR and LNT that used the Cu29Zn1/r-$Al_2O_3$ catalyst with 1% of Zn as a promoter, a cell density of 600 cpsi, and a volumetric ratio of 1.3 (SR/LNT). Finally, the NOx conversion was improved by about 20% compared to the LNT catalyst used alone.


## 1. Introduction

Recently, dimethyl ether (DME) has received increased attention as an alternative fuel for diesel engines. Since DME has an excellent self-ignition property, a high cetane number, and physical properties similar to those of LPG fuel, it can be used in most existing infrastructures, making it advantageous for commercialization. DME contains about 34.5% of oxygen ($O_2$); therefore, it has the advantage of exhausting only small particulate matter (PM) emissions compared to diesel engines. However, the diminishment of nitrogen oxide (NOx) emissions, which are slightly higher than those of diesel engines, is an important issue [1,2]. The Euro 6 regulations (effective in 2014) in Europe require a twofold decrease in NOx emissions for diesel passenger cars from the current limit of 0.18 g/km set by Euro 5 down to 0.08 g/km. Therefore, the after-treatment systems of motor vehicles will need to satisfy more stringent NOx emission standards in the future. Currently, de-NOx catalysts such as lean NOx trap (LNT), urea-selective catalytic reduction (SCR), and HC-SCR are well known [1,3]. Urea-SCR has been commercialized for passenger cars. However, it needs an alternative after-treatment system

* *Corresponding author*. Tel.: +82 62 530 1681; fax: +82 62 530 1689.
E-mail address: bcchoi@chonnam.ac.kr (B.C. Choi).
0360-3199/$ – see front matter 
doi:10.1016/j.ijhydene.2011.02.124

due to the large volume of the urea-SCR system and the associated inadequate infrastructure for supplying urea-aqueous solutions. On the other hand, the LNT catalyst has been commercialized for light commercial vehicles. Using a reductant (hydrogen ($H_2$), carbon monoxide (CO), or hydrocarbons (HCs)) that is obtainable from the post-injection of fuel without a special device, the NOx that is absorbed by the LNT catalyst can be effectively reduced [4]. In particular, $H_2$ is a more effective reductant of the LNT catalyst at low temperatures compared to other reductants. Furthermore, since DME has no sulfur, deactivation of the LNT catalyst by sulfur poisoning, which is a cause of performance deterioration of the LNT catalyst, does not occur [5]. DME steam reforming (SR) catalysts have been investigated with regard to copper (Cu)-based/r-$Al_2O_3$ catalysts in order to supply $H_2$ for fuel cells [6,7]. Many researchers have used various means to improve $H_2$ production such as the use of a Cu-based catalyst with transition metals as a promoter, the use of zeolite with a high acid site instead of r-$Al_2O_3$ [8], and the use of spinel-structure catalysts [9]; however, many problems have been reported including the low $H_2$ selectivity that is caused by the thermal aging and the side reactions of the SR catalyst [10,11]. Although the SR reaction needs an external heat source as it is endothermic, sources of heating have not been adequately considered. In order to apply the SR catalyst to DME engines, a monolithic honeycomb-type substrate must be coated with a washcoat. Since there is heat loss due to the volume of the catalyst, there will be a difference in temperature between the inlet and the outlet of the catalyst in an actual vehicle. We can estimate that there will be a slight difference in the DME conversion and the $H_2$ production between a substrate-loaded SR catalyst and a small amount of a powder catalyst. Meanwhile, the exhaust gas of the vehicle is wasted after clarification by an after-treatment system but the heat resource and the water vapor from the exhaust gas can be efficiently used because these are necessary for the SR reaction [12]. This has the effect of reducing the energy loss of the exhaust gases of vehicles. Fig. 1 shows the new concept of the combined system of SR and LNT proposed in this study. As far as possible, the SR catalyst should be located toward the exhaust manifold to easily supply heat and water vapor to the DME SR reaction. When DME is injected in a specific operating condition, $H_2$ is generated by the reaction of DME over the SR catalyst. The $H_2$ that is formed by the SR catalyst is then utilized by the LNT catalyst to reduce NOx in the exhaust gas [13]. Although the system is somewhat complicated, it may provide a way of lowering NOx emissions with negligible DME slip of the LNT catalyst. Currently, the DME SR catalyst for the generation of $H_2$ has to be improved, and a combined system of SR and LNT has to be developed; however, extant research is not sufficient [14].

This study was performed to develop a DME SR catalyst that can effectively generate $H_2$ by using the heat and the water vapor in the exhaust gases of vehicles. The final purpose of the study is the development of a combined system of SR and LNT using the $H_2$ and the CO that are generated in the DME SR catalyst in order to improve the performance of the de-NOx system.

## 2. Experimental details

### 2.1. *Preparation of catalysts*

The SR catalyst used in this experiment was prepared by the sol-gel method [14], and a commercialized LNT catalyst (Ordeg Co.; 400 cpsi (cell per square inch); cordierite) was used. The quantities of Cu loaded in the SR catalyst were 10, 20, 29, and 30 (metal; wt%) of the washcoat; further, zinc (Zn) was incorporated at 1 and 5% (metal; wt%) in the Cu-based catalyst. The specifications of the SR catalyst and the LNT catalyst are shown in Table 1. Aluminum isopropoxide (Al[OCH($CH_3$)$_2$]; Sigma–Aldrich; 99.9%) was dissolved in 100 ml of $H_2O$ at 60 °C. A proper quantity of the Cu precursor ([$Cu(NO_3)_2 2.5H_2O$]; Sigma–Aldrich) was added depending on the loaded quantity. After 30 min, 10 ml of ethylene glycol (Sigma–Aldrich; 99%) was injected, and the mixture was stirred for an hour. The pH was adjusted to two using $HNO_3$, and the mixture was stirred

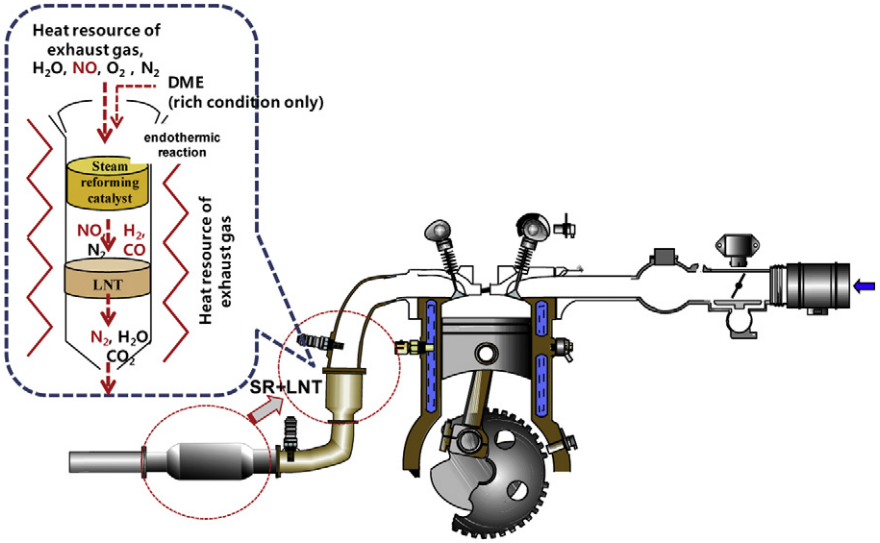


**Fig. 1 – Concept of the combined system of SR and LNT catalysts in order to improve the de-NOx performance.**

**Table 1 – Compositions of the wash coat manufactured by a sol-gel method and LNT catalyst commercialized.**

| Catalysts | BET ($m^2$/g) | Cu surface area ($m^2$/g) | Cu dispersion (%) |
|---|---|---|---|
| Cu10/r-$Al_2O_3$ | 272 | 0.34 | – |
| Cu20/r-$Al_2O_3$ | 265 | 0.96 | 21 |
| Cu30/r-$Al_2O_3$ | 259 | 1.43 | 45 |
| Cu29Zn1/r-$Al_2O_3$ | 243 | 1.66 | 65 |
| Cu25Zn5/r-$Al_2O_3$ | 234 | 1.33 | 43 |
| Catalyst | Composition (wt%) | | BET ($m^2$/g) |
| LNT | 1Pt/0.03Rh/0.02Pd | | 39.88 |

again for an hour. The solution was washed and then dried for 24 h at 130 °C. The washcoat was milled for two hours and then calcined for five hours at 500 °C. The calcined Cu-washcoat was dissolved in $H_2O$ and stirred for two hours for preparing the slurry. The substrate was dipped into the solution and then dried for 30 min at 200 °C under an air flow rate of 3 L/min. All the catalysts were calcined at 500 °C for two hours; they were then reduced with 10% of $H_2$ (balanced $N_2$) for six hours at 300 °C.

### 2.2. Experimental setup

A laboratory-scale model of a normal-pressure fixed-bed gas catalyst reactor was used to evaluate the reaction characteristics of the DME SR catalysts and the NOx conversion performance of the combined system of SR and LNT. The model gas catalyst reactor was composed by referring to a previous study [14]. The catalytic reactor used a cylindrical quartz tube with an inner diameter of 19 mm and a length of 350 mm. The catalysts were fixed at the center of the reaction tube and heated using an electric furnace. The catalyst temperatures in front of the SR catalyst (the $T_1$ point) and between the rear of the DME SR catalyst and the front of the LNT catalyst (the $T_2$ point) were measured using a 1.6 mm K-sheath thermocouple. The NOx concentration was analyzed by Fourier transform infrared spectroscopy (FT-IR; I2000; Midac). Hydrocarbons, DME, and $H_2$ were analyzed by a gas-chromatograph (GC; HP-6890; HP) with a flame ionization detector (FID) and a thermal conductivity detector (TCD). A Plot U column (Agilent) was used to measure the DME, and a molecular Sieve 5A column (Agilent) was used to measure the $H_2$, CO, and $CH_4$ with Ar carrier gas; further, the $CO_2$ was measured by a non-dispersive infrared (NDIR) analyzer (MEXA 554JK; Horiba).

### 2.3. Measurement of the $H_2$ and NOx conversions

The SR catalyst activity in terms of the $H_2$ yield was evaluated in the DME SR reaction at a space velocity (SV) ranging from 14,000 to 42,000 $h^{-1}$. The ratio of SR:LNT was, respectively, 2 (30 mm length for the SR catalyst), 1.3 (20 mm length for the SR catalyst), and 0.6 (10 mm length for the SR catalyst); DME was supplied continuously at 0.7%. The catalyst temperature was controlled by a temperature setting of either $T_1$ or $T_2$ in the electric furnace; however, in all the experiments, $T_2$ was selected as the catalyst temperature for analyzing the DME conversion and the $H_2$ yield [15]. The SR catalyst temperature varied in 50 °C intervals from 200 to 500 °C in steady conditions. The DME conversion of the SR catalyst was obtained from an equation, viz., "DME conversion (%) = $(1-[DME_{out}]/[DME_{in}]) \times 100$", by measuring the gas concentrations at the inlet and the outlet of the catalyst reaction part. The yield was obtained from the reactant gas production (%), viz., ("yield ratio of the reactant gases/yield ratio of $(H_2 + CO + CH_4 + CO_2)) \times$ DME conversion (%)". Before reaction, all the catalysts were reduced by 10% $H_2$ ($N_2$ balance) at each temperature in order to measure the $H_2$ yield under the same conditions. The LNT catalyst had a diameter of 18 mm and a length of 15 mm. The substrate cell density for the SR catalysts was selected as 400 and 600 cpsi, respectively, with regard to cordierite with a honeycomb-square type. For the combined system of SR and LNT, the SR catalyst was placed in front of the LNT catalyst, and the interval between the two catalysts was 7 mm. The NOx conversion was evaluated in a total flow rate of 2 L/min, as well as in conditions of 5% of $H_2O$, 10% of $O_2$, and 5% of $CO_2$. The balance gas was $N_2$. The experiment was carried out under a heating rate of 4 °C/min till 500 °C in the transient condition. Here, 0.7, 0.85 and 1% DME, respectively, was supplied as the reductant. The lean and rich conditions were maintained for 55 and 5 s, respectively. The SV of the LNT catalyst was 28,000 $h^{-1}$. The SV of the combined system of SR

**Table 2 – Evaluation conditions of catalytic activity.**

| Parameters | SR catalyst | LNT catalyst | | Combined system of SR + LNT catalyst | |
|---|---|---|---|---|---|
| Measurement | Reactant production | NOx conversion | | NOx conversion | |
| | | Lean | Rich | Lean | Rich |
| Temperature condition | Steady state | Transient | | Transient | |
| Total flow (L/min) | 2 | 2 | 2 | 2 | |
| SV ($h^{-1}$) | 14,000; 2,1000; 42,000 | 28,000 | | 9500; 12,000; 17000 | |
| DME (%) | 0.7 | 0 | 0.7, 0.85, 1 | 0 | 0.7 |
| $H_2O$ (%) | 5 | 5 | | 5 | |
| Balance gas | $N_2$ | $N_2$ | | $N_2$ | |
| $CO_2$ (%) | 0, 5 | 0, 5 | | 0, 5 | |
| NO (ppm) | 0 | 500 | 0 | 500 | 0 |
| $O_2$(%) | 0 | 10 | 0 | 10 | 0 |
| Size of catalyst (mm) | Diameter:19 Length:30; 20; 10 | Diameter:19 Length:15 | | SR + LNT | |
| Lean/rich time (sec) | Continuous | 55 | 8, 5, 2 | 55 | 5 |

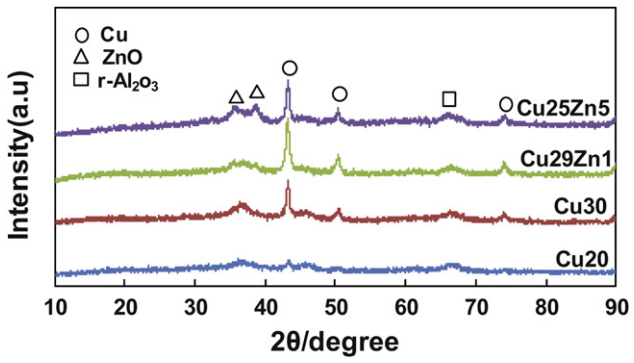


**Fig. 2 – XRD patterns of SR catalysts (Cu-based/r-$Al_2O_3$).**

and LNT varied depending on the length of the SR catalyst: 9,500 $h^{-1}$ (SR/LNT = 2); 12,000 $h^{-1}$ (1.3); and 17,000 $h^{-1}$ (0.6). Table 2 shows the detailed specifications of the experimental parameters. The NOx conversion of the combined system of SR and LNT was obtained from the equation, viz., "NOx conversion (%) = $(1-[NOx_{out}]/[NOx_{in}]) \times 100$".

### 2.4. *Characterization of the SR catalyst*

The measurement of the specific surface area of each catalyst used a physical adsorption method (the Brunauer–Emmett–Teller (BET) method) for measuring the $N_2$ gas adsorption quantity pursuant to the pressure change at the temperature of liquid nitrogen (77 K) after pretreatment in a $1 \times 10^{-6}$ Torr vacuum condition at 300 °C. The washcoat particles on the catalyst surface were observed by Transmission Electron Microscopy (TEM(×100k); JEM-2000FX2; Shimadzu). X-ray diffraction (XRD; D/MAX UltimaIII; Rigaku) analysis was carried out on the Y-2000 X-ray diffractometer using Cu–Ka radiation between $2\theta = 10°$ and 90°. The working conditions of the instrument were 40 kV and 40 mA. Temperature programmed reduction (TPR; BEL-CAT; BEL) experiments were performed with $H_2$ (5%) and He balance in a temperature range of 100–450 °C (ramping at 4 °C/min). The surface area and the dispersion of Cu were measured by nitrous oxide ($N_2O$) chemisorption; they could be obtained and calculated by quantifying the amount of $N_2O$ consumed by a 100 mg sample. After the catalyst was pre-reduced for four hours at 250 °C in 5% of $H_2$/Ar balance, it was exposed to a stream of He for 30 min at 250 °C and then cooled to the temperature for chemisorption. $N_2O$/He with a balance of 10% flowed for three hours (injection time: 10 min; injection loading time: 1 min). $N_2O$ decomposition on the exposed Cu surface was monitored by a gas-chromatograph equipped with a TCD.

## 3. Results and discussion

### 3.1. *Characteristics of the SR catalyst*

Fig. 2 shows the XRD pattern of the SR catalysts prepared by the sol-gel method for structural analysis. The Cu catalyst existed as CuO when the catalyst was produced in the sol-gel method but reverted to Cu after reduction with 10% $H_2$ for six hours. The Cu peak of Cu20/r-$Al_2O_3$ was weaker than that of Cu30/r-$Al_2O_3$. The greater was the Cu content, the greater the Cu intensity became. In the case of the Cu + Zn catalyst, Zn existed as ZnO on the SR catalyst because Zn is a type of transition metal that is more difficult to reduce compared to Cu [16].

Fig. 3 shows TEM images of the catalyst volume and the dispersion of Cu particles manufactured by the sol-gel method. As shown in Fig. 3(a)–(b), a higher content of Cu may benefit $H_2$ production but an excessively large amount of Cu degenerates dispersion. Fig. 3(b)–(d) show the particle sizes and dispersions of Cu30, Cu29Zn1, and Cu25Zn5/r-$Al_2O_3$, respectively. These figures also show that the addition of Zn as a promoter to the Cu catalyst decreases the Cu particle size and improves the dispersion [17]. This can imply that Zn as a promoter of the SR catalyst restricts the growth of Cu particles and improves their dispersion. Table 1 shows the BET surface area, the Cu surface area and the Cu dispersion of the catalyst produced in the sol-gel method. The BET surface area decreased as the amount of Cu was increased because the surface area of r-$Al_2O_3$, which contains 30% of Cu, became smaller. The BET surface area further decreased when Zn was added. On the other hand, the Cu surface area increased as the amount of Cu was increased. When the amount of Cu is increased, the reforming ability increases due to the increase

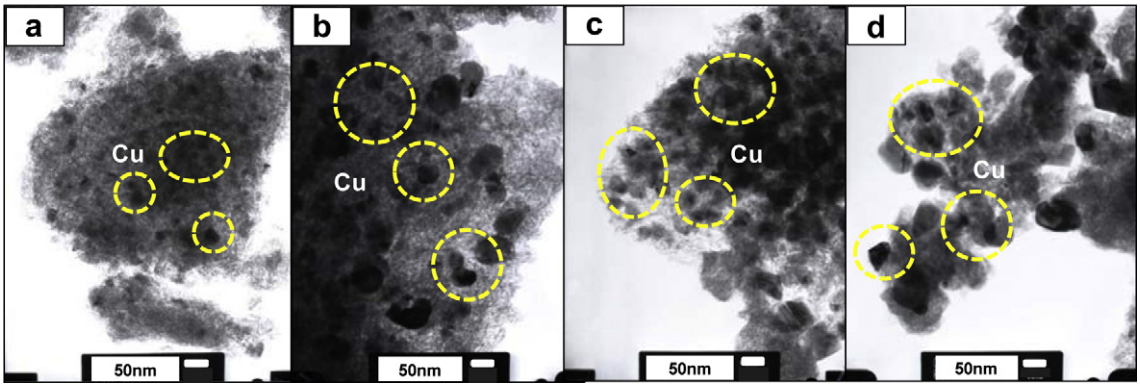


**Fig. 3 – TEM images of the washcoat manufactured by the sol-gel method ((a) Cu20/r-$Al_2O_3$, (b) Cu30/r-$Al_2O_3$, (c) Cu29Zn1/r-$Al_2O_3$, (d) Cu25Zn5/r-$Al_2O_3$).**

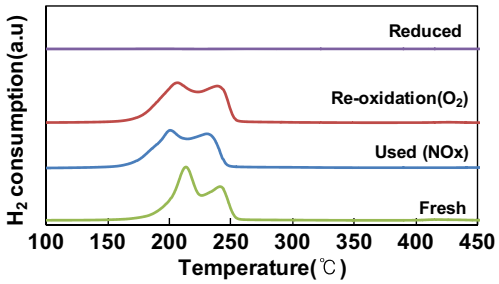


**Fig. 4 – $H_2$-TPR profiles of the Cu30/r-$Al_2O_3$ catalyst (Fresh: calcined catalyst; Reduced: catalyst after $H_2$ reduction; Re-oxidation: total flow rate 2 L/min, $O_2$ 10%, $H_2O$ 5%, $N_2$ balance and 200–500 °C; Used: total flow rate 2 L/min, DME 0.7%, NO 500 ppm, $O_2$ 10%, $H_2O$ 5%, $N_2$ balance, 200–500 °C).**

in the absolute amount of Cu; however, the Cu dispersion deteriorates partially due to the excess amount of Cu. Compared to Cu30/r-$Al_2O_3$, the Cu surface area of Cu29Zn1/r-$Al_2O_3$, which was augmented with 1% of Zn as a promoter, increased because the growth of Cu particles was restricted and the dispersion of Cu particles was improved [17,18]. By the inclusion of 1% of Zn, Cu, which is active in the DME SR reaction, can be increasingly dispersed; further, highly active Cu and $Cu^+$ can be kept stable. In the case of a catalyst that is prepared by the sol-gel method, a catalyst metal enters into a crystal and is supported under high dispersion by Zn; therefore, the condition of Cu can be kept stable [17,18]. Meanwhile, the Cu25Zn5/r-$Al_2O_3$ catalyst to which 5% of Zn was added became smaller than the Cu30/r-$Al_2O_3$ catalyst. Thus, 1% of Zn was more beneficial than 5% of Zn for increasing the surface area and the dispersion of Cu because an excessive bond of Zn–Zn causes the agglutination of Cu particles.

Fig. 4 shows the TPR profiles of the catalysts produced by calcination of the SR catalyst (Cu30/r-$Al_2O_3$). Excessive $O_2$ and NOx are emitted from the exhaust gases of vehicles that operate in lean conditions. In particular, the Cu of the Cu-based SR catalyst can react with the excess $O_2$ and re-oxidize to CuO. Therefore, in order to apply the SR catalyst to a commercial exhaust gas treatment system for DME vehicles, the reductive performance is important. The TPR profiles show no TPR peak in the reduced catalyst. This agrees with the XRD peak in Fig. 2. The re-oxidation catalyst was oxidized to CuO by the coupling of $O_2$ with Cu, and the reduction started at about 180 °C and finished at about 250 °C. The used catalyst showed a similar peak as the re-oxidation catalyst. Reduction regarding the first-peak of NOx started at about 170 °C, and the peak appeared at about 200 °C. The second-peak appeared at about 230 °C and finished at about 250 °C. The formation of the first-peak is due to the reduction of isolated $Cu^{2+}$ ions and copper oxide clusters. The formation of the second-peak is due to the reduction of large copper oxide clusters and the bulk CuO phase [19,20]. It has been reported that $O_2$, which is supplied in a lean condition, oxidizes to CuO through coupling with the Cu of the reduced catalyst; however, in a rich condition, CuO reduces back to Cu because $H_2$ is generated by the reaction of the injected DME after the blocking of $O_2$ [21]. However, this effect was not great in the results of this experiment. It appears that the effects of $O_2$ and NO on the reductive performance of the SR catalyst were not great either because the SR catalyst does not absorb NO (see Fig. 5). According to the results of the TPR experiment, CuO returns to Cu below 250 °C; hence, activation of the SR catalyst is expected after 250 °C even in the vehicle exhaust gas condition.

### 3.2. NOx conversion of the LNT catalyst

Fig. 5 shows the experimental results regarding the NOx absorption performance of the LNT catalyst and the combined system of SR and LNT. The NOx conversion of the LNT catalyst is determined by the NOx absorption performance and the reactivity of the reductant. The NOx absorption performance in the catalyst is impacted by the cohesion between particles due to the van der Waals forces and the chemical binding between the adsorbent and the absorbed matter [22]. In the LNT catalyst, NOx is absorbed in the lean condition but the absorbed NOx is separated by the injected reductant in the rich condition. Therefore, the absorption performance has a dominant influence on the total NOx emission characteristics. Even though the LNT catalyst has the highest NOx absorption volume, its highest NOx conversion appears between 300 and 350 °C due to the Pt activation temperature [23]; the LNT catalyst used in this experiment exhibited very different features. The Pt on the LNT catalyst used in this experiment was considerably activated at 200 °C, and more than 60% of NO was oxidized to $NO_2$ (Fig. 5 is not shown); further, the absorption volume was the highest at this time. As the temperature rose, the NOx absorption capacity decreased more because the LNT catalyst was separated without absorbing NOx at high temperatures. The combined system of SR and LNT also showed a similar absorption performance as the LNT catalyst over the entire temperature range. The NOx absorption performance of the SR catalyst was found to be small because NOx is stored as $Ba(NO_3)_2$ when only the LNT catalyst is used.

Fig. 6 shows the NOx conversion and the DME slip in relation to the DME injection quantity (0.7, 0.85, and 1%), and

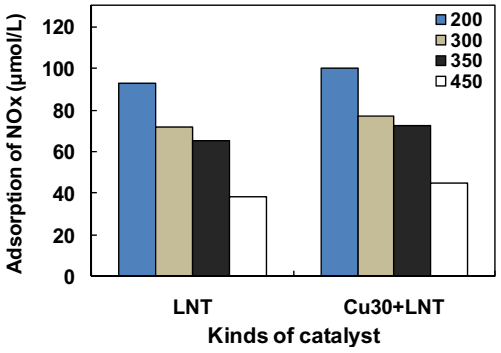


**Fig. 5 – Adsorption of NOx on the LNT catalyst and the combined system of SR and LNT catalysts (Total flow rate 2 L/min, NO 500 ppm, $O_2$ 10%, $N_2$ balance, SR catalyst: SR/LNT = 2, 400 cpsi).**

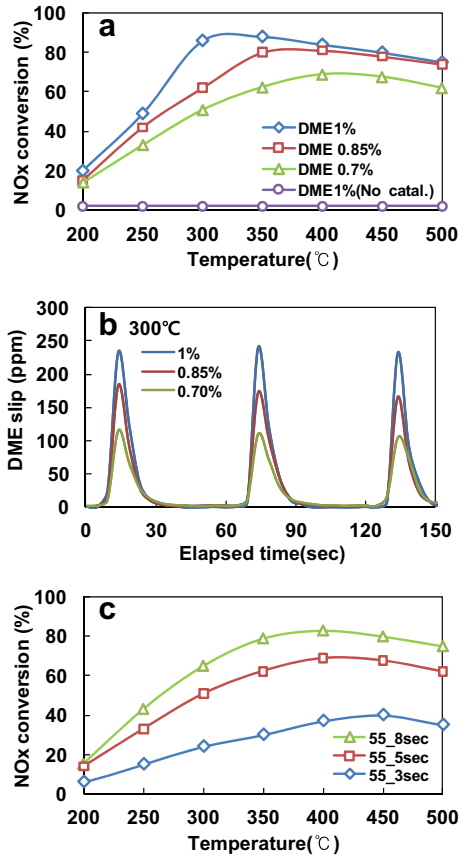


**Fig. 6 – (a, c) NOx conversion and (b) concentration of the DME slip, according to the amount and injection quantity and time of DME (Total flow rate 2 L/min, DME 0.7%, NO 500 ppm, $O_2$ 10%, $H_2O$ 5%, $N_2$ balance, transient condition, LNT catalyst: SV = 28000 $h^{-1}$).**

injection time (3, 5, and 8 sec). The LNT catalyst showed the largest absorption quantity at 200 °C (see Fig. 5) but the NOx conversion was relatively low because the reactivity of DME is low. As shown in Fig. 6(a), the NOx conversion was 60, 80, and 85% at 350 °C, when the DME supply was 0.7, 0.85, and 1%, respectively. At the same time, the variation in the NOx conversion with the DME supply was about 25%.

DME decomposition:

$$CH_3OCH_3 \rightarrow H_2 + CO_2 + CH_4 \quad (1)$$

Furthermore, in the absence of catalysts (either SR or LNT), the NOx conversion was almost zero because $H_2$ was not produced by DME decomposition (Eq. (1)). For the DME slip in Fig. 6(b), the highest NOx conversion was obtained when 1% of DME was supplied over the entire temperature range but the highest DME slip also occurred at 300 °C. Fig. 6(c) shows the NOx conversion when the lean/rich time (periodic pulse) was changed to 55/3, 55/5, and 55/8 s, respectively, with 0.7% of DME. The highest NOx conversion was obtained at the lean/rich time of 55/8 s, wherein the quantity of DME supply was the largest in the intermediate condition. Consequently, it was found that even though the NOx conversion increased as the injection quantity and the time regarding DME usage as a reductant increased, the DME slip also increased at the rear of the LNT catalyst. Therefore, we determined that 0.7% of DME supply and 55/5 s of the injection time were advantageous for the combined system of SR and LNT considering the fuel penalty of DME vehicles [24] and the DME slip. Thereafter, the supply quantity and the lean/rich injection time of DME were selected as 0.7% and 55/5 s, respectively, for all experiments.

### 3.3. *DME conversion over the SR catalyst*

Fig. 7(a)–(b) show the temperature profiles and Fig. 7(c) shows the DME conversion in relation to the temperature setting of the electric furnace. The volumetric ratio between the SR and LNT catalysts (SR/LNT) was 2, and the cell density of the substrate was 400 cpsi. The inlet temperature ($T_1$) of the SR catalyst was the same as the outlet temperature ($T_2$) without reaction flow but the two temperatures differed under only DME flow (no SR catalyst). Fig. 7(a) shows the temperature profiles when the temperature setting of the furnace was $T_1$. The value of $T_2$ in the DME flow condition and with the SR (Cu30/r-$Al_2O_3$) catalyst was higher than that of $T_1$ because the electric furnace supplied more power as $T_1$ decreased due to the endothermic reaction of DME in front of the SR catalyst

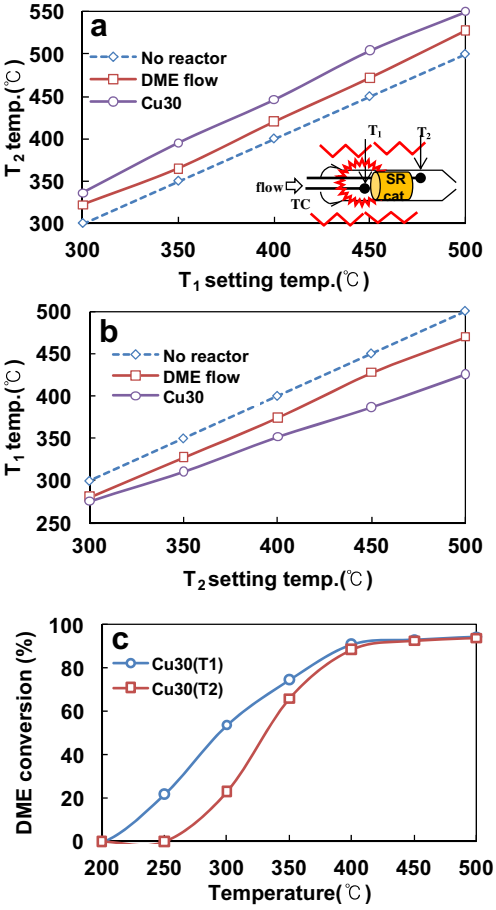


**Fig. 7 – DME conversion according to the temperature setting (SV 14000 $h^{-1}$, Total flow rate 2 L/min, DME 0.7%, $H_2O$ 5%, $N_2$ balance, steady state condition, SR catalyst: SR/LNT = 2, 400 cpsi).**

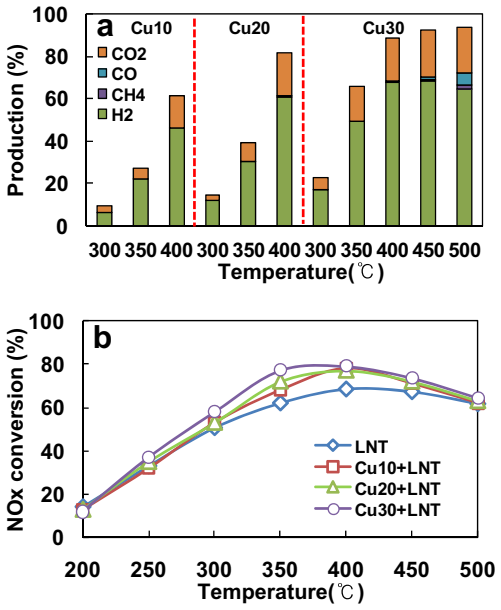


**Fig. 8 – (a) $H_2$ production of the SR catalyst and (b) NOx conversion of the combined system of SR and LNT catalysts according to the Cu loading (Total flow rate 2 L/min, DME 0.7%, NO 500 ppm, $O_2$ 10%, $H_2O$ 5%, $N_2$ Balance, 55/5 s (rich/lean time), SR catalyst: SR/LNT = 2, 400 cpsi).**

[25]. $T_1$ required a large heat source to rise up to the temperature setting. On the other hand, Fig. 7(b) shows the temperature profiles when the temperature setting of the furnace was $T_2$. The value of $T_1$ in the DME flow condition and with the SR (Cu30/r-$Al_2O_3$) catalyst was lower than that of $T_1$ because the electric furnace supplied less heat as the $T_2$ temperature setting was higher than $T_1$.

Fig. 7(c) shows the DME conversion in relation to the temperature settings of the furnace. The DME conversion under the $T_1$ temperature setting was higher in the range of 200–400 °C than under the $T_2$ temperature setting. Considering actual application to vehicles of the combined system of SR and LNT, the $T_2$ temperature setting, which can control the appropriate temperature of the SR and LNT catalysts, was more similar to the actual vehicle condition than $T_1$. This is because the $T_1$ temperature setting was forced by much of the heat resource to rise up. Although the DME conversion of the SR catalyst decreased, the $T_2$ point was determined as the catalyst temperature for evaluating the DME conversion and/or the de-NOx performance of the catalysts.

### 3.4. *NOx conversion of the combined system of SR and LNT*

Fig. 8(a)–(b), respectively, show the $H_2$ production and the NOx conversion in relation to the Cu loading of the SR catalysts (Cu10, 20, 30/r-$Al_2O_3$) in the combined system of SR and LNT. The volumetric ratio between the SR and LNT catalysts was 2, and the cell density was 400 cpsi. As shown in Fig. 8(a), the $H_2$ production for three types of SR catalyst, viz., Cu10, 20, and 30/r-$Al_2O_3$ was 22, 30, and 58%, respectively, at 350 °C. Of the three SR catalysts, the highest $H_2$ production was obtained over Cu30/r-$Al_2O_3$ because it had the largest amount of Cu. In the light of $H_2$ production, a Cu catalyst using steam reforming initiates the DME hydrolysis, methanol steam reforming, and steam reforming reactions as follows [8,10].

DME hydrolysis:

$$CH_3OCH_3 + H_2O \rightarrow 2CH_3OH \quad (2)$$

Methanol steam reforming:

$$CH_3OH + H_2O \rightarrow 3H_2 + CO_2 \quad (3)$$

DME steam reforming:

$$CH_3OCH_3 + 3H_2O \rightarrow 6H_2 + 2CO_2 \quad (4)$$

DME is hydrolyzed by r-$Al_2O_3$ to methanol (Eq. (2)), and this methanol is reformed to generate $H_2$ (Eq. (3)) by Cu. Therefore, a larger amount of Cu is more advantageous for $H_2$ production. It was reasoned that 30% of Cu was the most appropriate amount in this experiment because a larger amount of Cu deteriorates the dispersion property [14]. From the perspective

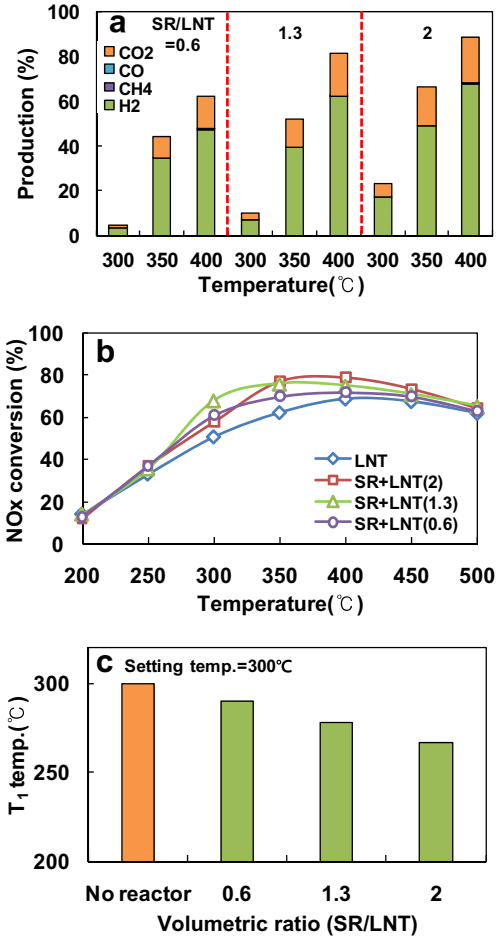


**Fig. 9 – Effect of the volumetric ratio of the SR catalyst on (a) $H_2$ production and (b) NOx conversion of the combined system of SR and LNT catalysts (Total flow rate 2L/min, DME 0.7%, NO 500 ppm, $O_2$ 10%, $H_2O$ 5%, $N_2$ Balance, 55/5 s, SR catalyst: 400 cpsi, SR/LNT = 0.6(SV = 42,000 $h^{-1}$), 1.3 (21,000 $h^{-1}$), 2(14,000 $h^{-1}$)).**

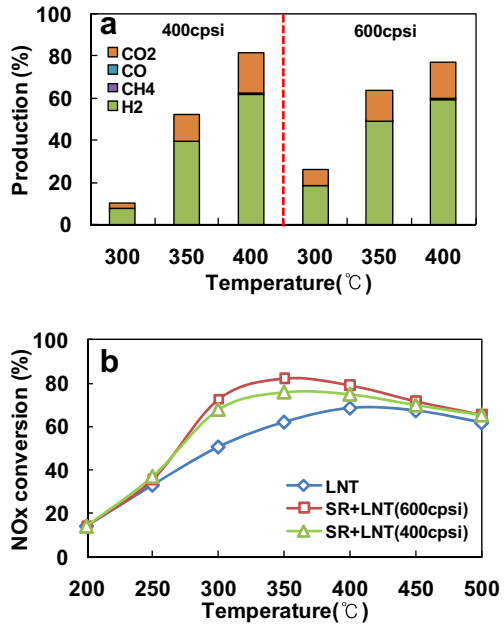


**Fig. 10 – Effect of cell the density of the substrate on (a) $H_2$ production and (b) NOx conversion of the combined system of SR and LNT catalysts (Total flow rate 2 L/min, DME 0.7%, NO 500 ppm, $O_2$ 10%, $H_2O$ 5%, $N_2$ Balance, 55/5 s, SR catalyst: SR/LNT = 1.3).**

of $H_2$ production, the optimum amount of Cu may vary with the catalyst preparation method. $H_2$ production was over 70% at 400 °C for Cu30/r-$Al_2O_3$. It was found that the higher the temperature was, the higher the $H_2$ production became; however, it was observed that the production of $H_2$ gradually decreased and that of CO increased at temperatures over 450 °C due to the reverse water shift reaction [21]. In a lot of studies, DME has been reported as a hydrogen carrier to supply $H_2$ to fuel cells. In this case, the generation of CO is undesirable for the purpose of supplying pure $H_2$ to fuel cells [26] but the production of a small amount of CO besides $H_2$ is also useful as a reductant for the combined system of SR and LNT. Furthermore, for the DME SR reaction, even though higher NOx conversion was expected from the combined system of SR and LNT at high temperatures as higher catalyst temperatures are advantageous for $H_2$ production, the NOx conversion decreased at temperatures over 400 °C because the NO absorption of the LNT catalyst was small in high-temperature regions [23].

Fig. 9(a) shows the effect of the volumetric ratio between the SR and LNT catalysts on the $H_2$ production of the SR catalyst, while Fig. 9(b) depicts the NOx conversion in the combined system of SR and LNT. For the results described above, Cu30/r-$Al_2O_3$ was used as the SR catalyst because it showed the largest $H_2$ production among the Cu-based catalysts. As shown in Fig. 9(a), the volumetric ratio between the SR and LNT catalysts was 0.6 (SV = 42,000 $h^{-1}$), 1.3 (21,000 $h^{-1}$), and 2 (14,000 $h^{-1}$), respectively, and the $H_2$ production of the SR catalyst was 5, 8, and 21%, respectively, at 300 °C and 48, 64, and 72%, respectively, at 400 °C. Thus, the bigger the volume of the SR catalyst was, the greatest was the $H_2$ production. This is because the residence time of DME for reaction on the catalyst increased during the SR reaction. As shown in Fig. 9(b), the highest NOx conversion was realized under SR/LNT = 1.3 at 300 °C and SR/LNT = 2 above 350 °C. As shown in Fig. 9(c), the $T_1$ temperature was 290, 277, and 262 °C, respectively, under different volumetric ratios of SR/LNT, when the temperature ($T_2$) setting of the catalyst was 300 °C. Thus, the smaller the volumetric ratio of the SR/LNT was, the higher the $T_1$ temperature became. This is because non-reacted DME on the SR catalyst was oxidized on the LNT catalyst, and the heat generated by the exothermic reaction of DME transferred to the SR catalyst. In this case, as the volume of the SR catalyst increased, the heat capacity of the SR catalyst increased and $T_1$ decreased. Thus, the SR/LNT of 1.3 is appropriate for the combined system of SR and LNT. As shown above, the development of the SR catalyst for more $H_2$ production is important for the optimization of the combined system of SR and LNT.

Fig. 10(a) shows the effect of the cell density of the substrate on the $H_2$ production of the SR catalyst, while Fig. 10 (b) presents the NOx conversion of the combined system of SR and LNT. As shown in Fig. 10(a), the $H_2$ production of the SR catalyst under 400 cpsi was 10, 40, and 60%, respectively, at 300, 350, and 400 °C. On the other hand, the $H_2$ production of the SR catalyst under 600 cpsi was 20, 50, and 60% at 300, 350, and 400 °C, respectively. Thus, the $H_2$ production of the SR catalyst under 600 cpsi was slightly higher than that under 400 cpsi. As shown in Fig. 10(b), the NOx conversion in the combined system of SR and LNT under cell densities of 400 and 600 cpsi, respectively, was 75 and 85% at 350 °C. The combined system of SR and LNT using the 600 cpsi SR catalyst also had a higher NOx conversion because of the high $H_2$ production of the SR catalyst under 600 cpsi compared to that of the SR catalyst under 400 cpsi. This is because the cell density of 600 cpsi features a higher surface area than that of

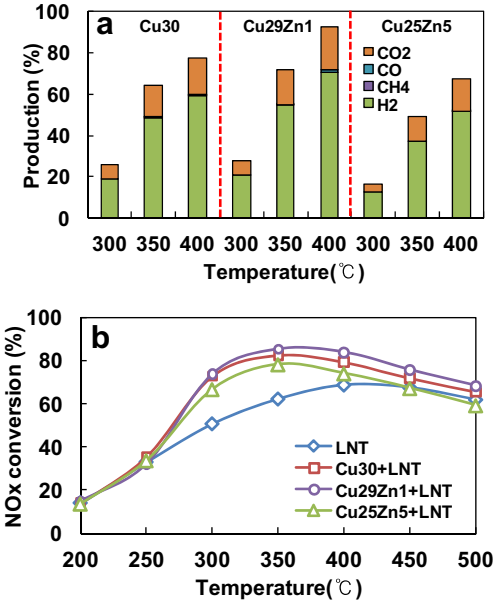


**Fig. 11 – (a) Effect of Zn promoter on $H_2$ production, and (b) NOx conversion of the combined system of SR and LNT catalysts (Total flow rate 2 L/min, DME 0.7%, NO 500 ppm, $O_2$ 10%, $H_2O$ 5%, $N_2$ Balance, 55/5 s, SR catalyst: SR/LNT = 1.3, 600cpsi).**

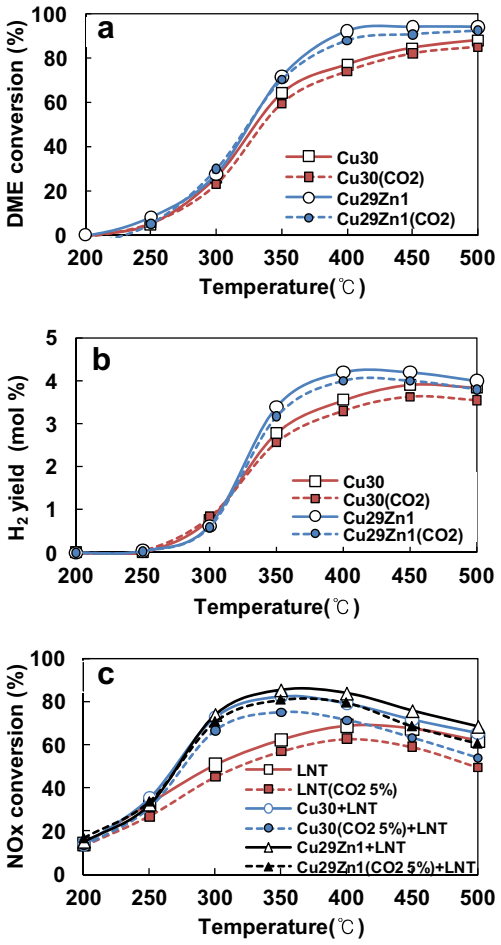


**Fig. 12 – Effect of the $CO_2$ presence (5%) on (a) DME conversion, (b) $H_2$ yield and (c) NOx conversion of the combined system of SR and LNT catalysts (Total flow rate 2 L/min, DME 0.7%, NO 500 ppm, $O_2$ 10%, $CO_2$ 5%, $H_2O$ 5%, $N_2$ Balance, 55/5 s, SR catalyst: SR/LNT = 1.3, 600 cpsi).**

400 cpsi, which means a greater frequency of reaction on the catalyst with the reaction gases. In line with the aforementioned results of the prior experiment, the SR catalysts for all subsequent experiments were prepared with a cell density of 600 cpsi and a volumetric ratio of 1.3 for SR/LNT.

Fig. 11(a) shows the effect of Zn as a promoter on the $H_2$ production of the SR catalysts, while Fig. 11(b) presents the NOx conversion in the combined system of SR and LNT. Zn, which is a transition metal, was mixed with the Cu-based SR catalyst as a promoter for Cu dispersion at 1 and 5%. As shown in Fig. 11(a), the $H_2$ production of Cu30, Cu29Zn1, and Cu25Zn5/r-$Al_2O_3$ was 48, 54, and 37%, respectively, at 350 °C, and 59, 70, and 51%, respectively, at 400 °C. The descending order of $H_2$ production in the SR catalysts was Cu29Zn1 > Cu30 > Cu25Zn5/r-$Al_2O_3$. As mentioned above, the addition of 1% of Zn improved the dispersion of Cu and increased the surface area and the dispersion of Cu [27]. On the other hand, Cu25Zn5/r-$Al_2O_3$ to which 5% of Zn was added showed lower $H_2$ production compared to Cu30/r-$Al_2O_3$. This is because the addition of 5% of Zn did not improve the surface area and the dispersion of Cu particles, and the loaded amount of Cu was lower than that of Cu30/r-$Al_2O_3$ (as seen in Fig. 3). Therefore, as shown in Fig. 11(b), the highest NOx conversion was 83% at 350 °C for the combined system of Cu29Zn1/r-$Al_2O_3$ and LNT. This system featured an improvement of 20% in the NOx conversion compared with the LNT catalyst. The NOx conversion of the combined system of SR (Cu29Zn1/r-$Al_2O_3$) and LNT improved slightly compared with that of the system of Cu30/r-$Al_2O_3$ and LNT.

Fig. 12(a) shows the effect of $CO_2$ coexistence on DME conversion, Fig. 12(b) represents the $H_2$ production of the SR catalyst, and Fig. 12(c) illustrates the NOx conversion of the combined system of SR and LNT. Component gases that can be generated by reforming DME in the SR catalyst include $H_2$, $CO_2$, and CO. Among them, $H_2$ and CO can be useful reductants for the LNT catalyst but $CO_2$ can restrict the activation of this catalyst [28]. As the exhaust emissions from lean burn engines also contain $CO_2$ of 5–10%, this was simulated for the experiments. Therefore, the effect of $CO_2$ on the combined system needs to be investigated. Fig. 12(a) shows that DME conversions under the coexistence of 5% of $CO_2$ were lowered by about 5% for both Cu30/r-$Al_2O_3$ and Cu29Zn1/r-$Al_2O_3$ over the entire temperature range. However, 90% or higher DME conversion was obtained at over 400 °C regardless of the coexistence of $CO_2$. As shown in Fig. 12(b), the $H_2$ production was not much affected by the coexistence of $CO_2$. The $H_2$ production under the Cu29Zn1/r-$Al_2O_3$ catalyst decreased by approximately 0.5% at 400 °C and 450 °C. However, a DME conversion of 90% or higher could be obtained even above 400 °C regardless of the coexistence of $CO_2$. In general, 6 mol of $H_2$ are generated when 1 mol of DME reacts in the SR reaction (Eq. (4)). Fig. 12(c) shows the variation of the NOx conversion with the coexistence of 5% of $CO_2$ in the reactant gases. The NOx conversions of all kinds of catalyst decreased by 5–10% under the coexistence of $CO_2$. The NOx conversion of the LNT catalyst decreased by 5–10% under the coexistence of $CO_2$. The combined system of SR and LNT using the Cu29Zn1/r-$Al_2O_3$ catalyst showed a NOx conversion of about 80% (at 350 °C) under the coexistence of $CO_2$. The NOx conversion of the system with Cu29Zn1/r-$Al_2O_3$ decreased by about 5% under the coexistence of $CO_2$. In the LNT catalyst, NOx is stored in $Ba(NO_3)_2$ without $CO_2$. Under the coexistence of $CO_2$, however, NOx is stored in r-$Al_2O_3$ and $BaCO_3$; thus, the NOx conversion of the LNT catalyst decreases due to the deactivation of the Ba site [28]. Therefore, $CO_2$ suppresses NOx storage in the LNT catalyst; further, in the present experiment, the NOx conversion decreased due to increasing NOx desorption when DME was supplied in a rich condition. As a result, the NOx conversion in the combined system of SR and LNT also decreased by about 5–10%.

## 4. Conclusions

This study was performed to develop a DME SR catalyst with high $H_2$ production using the heat source and water in the exhaust emissions of vehicles so as to supply $H_2$ as a reductant of the LNT catalyst and optimize the combined system of SR and LNT catalysts using the $H_2$ and CO generated from the DME SR catalyst in order to improve the performance of the

de-NOx catalyst. The following conclusions were obtained as the results of this study.

Of the DME SR catalysts produced by the sol-gel method, the highest DME conversion and $H_2$ production were realized over the Cu30/r-$Al_2O_3$ catalyst. The higher the temperature was, the more the $H_2$ production became; however, the $H_2$ production decreased and the CO production increased at temperatures above 450 °C due to the reverse water shift reaction. The bigger the volume of the catalyst was, the more the DME conversion and the $H_2$ production became; further, the SR catalyst using the 600 cpsi substrate exhibited the most $H_2$ production. This is because the 600 cpsi substrate with a higher cell density contains more of the washcoat than the 400 cpsi substrate, and the catalyst has more opportunities to react with the reactant gases. Furthermore, the highest NOx conversion and $H_2$ production were shown over the combined system of SR and LNT using the Cu29Zn1/r-$Al_2O_3$ catalyst that included 1% of Zn as a promoter. The combined system of SR and LNT using Cu29Zn1/r-$Al_2O_3$ as the SR catalyst with a volumetric ratio (SR/LNT) of 1.3 and a cell density of 600 cpsi improved the NOx conversion by about 20% at temperatures above 300 °C compared to that of the LNT catalyst used solely. This is because the $H_2$ and some CO generated from the DME SR catalyst were used as reductants for the LNT catalyst. We expected that the combined system of SR and LNT using the ratio of SR/LNT = 2 with the highest $H_2$ production would be the most advantageous for NOx conversion but the highest NOx conversion was seen at the ratio of SR/LNT = 1.3. The coexistence of 5% of $CO_2$ in the reactant gases decreased the NOx conversion of the combined system of SR and LNT but this was influenced more by the deactivation of the LNT catalyst than that of the SR catalyst. The SR catalyst could be reduced to Cu at 250 °C even in the exhaust gases of the DME vehicle. Therefore, the NOx conversion of the combined system of SR and LNT could be improved further if we could develop a DME SR catalyst that had high $H_2$ production at 250 °C.

## Acknowledgements

This work was financially supported by a grant from the Industrial Source Technology Development Program (10033505 200911) of the Ministry of Knowledge Economy (MKE) of Korea.

## REFERENCES

[1] Sitshebo S, Tsolakis A, Theinnoi K. Promoting hydrocarbon-SCR of $NO_x$ in diesel engine exhaust by hydrogen and fuel reforming. Int J Hydrogen Energy 2009;34:7842–50.
[2] Tsolakis A, Megaritis A. Partially premixed charge compression ignition engine with on-board $H_2$ production by exhaust gas fuel reforming of diesel and biodiesel. Int J Hydrogen Energy 2005;30:731–45.
[3] Saravanan N, Nagarajan G. An insight on hydrogen fuel injection techniques with SCR system for $NO_x$ reduction in a hydrogen–diesel dual fuel engine. Int J Hydrogen Energy 2009;34:9019–32.
[4] Sedlmair CH, Seshan K, Jentys A, Lercher JA. Elementary steps of $NO_x$ adsorption and surface reaction on a commercial storage–reduction catalyst. J Catal 2003;214:308–16.
[5] Nishioka H, Yoshida K, Asanuma T, Fukuma T. Development of clean diesel $NO_x$after-treatment system with sulfur trap catalyst. SAE 2010; 2010-01-3030.
[6] Wang X, Pan X, Lin R, Kou S, Zou W, Ma J. Steam reforming of dimethyl ether over Cu–Ni/$\gamma$-$Al_2O_3$ bi-functional catalyst prepared by deposition-precipitation method. Int J Hydrogen Energy 2010;35:4060–8.
[7] Takeishi K, Suzuki H. Steam reforming of dimethyl ether. Appl Catal A Gen 2004;260:111–7.
[8] Faungnawakij K, Tanaka Y, Shimoda N, Fukunaga T, Kawashima S, Kikuchi R, et al. Influence of solid–acid catalysts on steam reforming and hydrolysis of dimethyl ether for hydrogen production. Appl Catal A Gen 2006;304:40–8.
[9] Faungnawakij K, Kikuchi R, Fukunaga T, Eguchi K. Catalytic hydrogen production from dimethyl ether over $CuFe_2O_4$ spinel-based composites: hydrogen reduction and metal dopant effects. Catal Today 2008;138:157–61.
[10] Fukunaga T, Ryumon N, Shimazu S. The influence of metals and acidic oxide species on the steam reforming of dimethyl ether (DME). Appl Catal A Gen 2008;348:193–200.
[11] Faungnawakij T, Kikuchi R, Matsui T, Fukunaga T, Eguchi K. A comparative study of solid acids in hydrolysis and steam reforming of dimethyl ether. Appl Catal A Gen 2007;333:114–21.
[12] Kašpar J, Fornasiero P, Hickey N. Automotive catalytic converters: current status and some perspectives. Catal Today 2003;77:419–49.
[13] Betta C, Sheridan D, Cizeron J. Diesel engine emissions reduction (DEER) conference. Coronado, California; 2004.
[14] Park SY, Kim HN, Choi BC. Effective parameters for DME steam reforming catalysts for the formation of $H_2$ and CO. J Ind Eng Chem 2010;16:734–40.
[15] Park SY, Kim HN, Choi BC. Hydrogen production by steam reforming (SR) of DME over Cu catalysts and de-$NO_x$ performance of a combined system of SR + LNT. Catal Today, in press.
[16] Monti DM, Cant NW, Trimm DL, Wainwright MS. Hydrogenolysis of methyl formate over copper on silica: I. Study of surface species by in situ infrared spectroscopy. J Catal 1986;100:17–27.
[17] Feng D, Wang Y, Wang D, Wang J. Steam reforming of dimethyl ether over CuO–ZnO–$Al_2O_3$–$ZrO_2$ ± ZSM-5: a kinetic study. Chem Eng J 2009;146:477–85.
[18] Takeishi K, Yamamoto K. Dimethyl ether steam reforming catalyst and method for producing the same. US Patent 2004: A1. US 2004/0192547.
[19] Dow WP, Wang YP, Huang TJ. Yttria-stabilized zirconia supported copper oxide catalyst. J Catal 1996;160:155–70.
[20] Dow WP, Huang TJ. Effect of chlorine on TPR and TPO behavior of an YSZ/r-$Al_2O_3$ supported copper oxide catalyst. Appl Catal A Gen 1996;141:17–29.
[21] Faungnawakij K, Tanaka Y, Shimoda N, Fukunaga T, Kikuchi R, Eguchi K. Hydrogen production from dimethyl ether steam reforming over composite catalysts of copper ferrite spinel and alumina. Appl Catal B Enviro 2007;74:144–51.
[22] Jun HJ, Seo G. An introduction to catalyst. Seoul, Korea: Hanlimwon; 1995. p. 15–54.
[23] Epling WS, Campbell LE, Yezerets A, Currier NW, Parks II JE. Overview of the fundamental reactions and degradation mechanisms of $NO_x$ storage/reduction catalysts. Catal Revi Sci Eng 2004;46:163–245.

[24] Papadakis K, Odenbrand CU, Sjoblom J, Creaser D. Development of a dosing strategy for a heavy-duty diesel exhaust cleaning system based on $NO_X$ storage and reduction technology by design of experiments. Appl Catal B Enviro 2007;70:215–25.
[25] Faungnawakij K, Viriya-empikul N. Catalytic behavior toward oxidative steam reforming of dimethyl ether over $CuFe_2O_4$–$Al_2O_3$ composite catalysts. Appl Catal A Gen 2010; 382:21–7.
[26] Adams WA, Blair J, Bullock KR, Gardner CL. Enhancement of the performance and reliability of CO poisoned PEMfuel cells. J Pow Source 2005;145:55–61.
[27] Wu GS, Mao DS, Lu GZ, Cao YC, Fan KN. The role of the promoters in Cu based catalysts for methanol steam reforming. Catal Lett 2009;130:177–84.
[28] Scholz CML, Gangwal VR, de Croon MHJM, Schouten JC. Influence of $CO_2$ and $H_2O$ on $NO_x$ storage and reduction on a Pt–Ba/r-$Al_2O_3$ catalyst. Appl Catal B Enviro 2007;71:143–50.